Journal of Applied Biology & Biotechnology Vol. 14(1), pp. 135-142, January-February, 2026

Available online at http://www.jabonline.in

DOI: 10.7324/JABB.2025.259214



Eco-friendly fabrication of silver nanoparticles from the red macroalga *Scinaia moniliformis* and evaluation of their biomedical activities

Hemangiben Sheth*, Charumati Jha

Department of Botany, Smt. S. M. Panchal Science College, Talod, Gujarat, India.

ARTICLE INFO

Article history: Received on: 19/05/2025 Accepted on: 22/08/2025 Available online: 25/11/2025

Key words: Red macroalga, Silver nanoparticles, Antioxidant, Antibacterial, Anticancer

ABSTRACT

The present study reports the green synthesis of silver nanoparticles (AgNPs) using the red macroalga *Scinaia moniliformis* J. Agardh, an underexplored marine species rich in bioactive compounds. This eco-friendly method utilized the aqueous algal extract as a natural hydrophilic reducer and stabilizer. A visible color shift from light yellow to dark brown signified AgNP formation, which was further confirmed by characterization techniques including UVVis spectroscopy, FTIR, XRD, and TEM-SAED. A distinct surface plasmon resonance peak at 437 nm confirmed nanoparticle synthesis, while XRD validated their crystalline nature. FTIR indicated the presence of phenolics, proteins, and other biomolecules involved in reduction and capping. TEM analysis revealed predominantly spherical nanoparticles with an average size of 24.03 nm. Functionally, the AgNPs displayed strong antibacterial activity against both Gram-positive and Gram-negative bacteria, with the highest inhibition against *Escherichia coli* and *Shigella dysenteriae*. They also exhibited potent, dose-dependent antioxidant activity (IC50 = 41.09 \pm 0.35 μ g) and significant cytotoxicity against MCF-7 breast cancer cells (IC50 = 51.49 \pm 0.45 μ g). These findings underscore the novelty of using *S. moniliformis* for nanoparticle synthesis and highlight the broad biomedical applicability of the resulting AgNPs in antimicrobial and anticancer therapeutics.

1. INTRODUCTION

The advancement of nanotechnology has brought significant progress across various scientific disciplines, including medicine, environmental science, and materials engineering. Among the diverse nanomaterials developed, metallic nanoparticles — particularly silver nanoparticles (AgNPs) — have gained considerable attention due to their unique physicochemical properties and broad-spectrum biological activities. Conventionally, metallic nanoparticles are synthesized through physical and chemical methods; however, these techniques often require high energy input and involve toxic solvents or hazardous reducing agents, which raise concerns about environmental sustainability and biological safety [1,2].

In recent years, green synthesis of nanoparticles has emerged as a promising alternative to conventional methods. This environmentally benign approach employs biological systems such as plants, fungi, bacteria, and algae as natural reducing and stabilizing agents [3]. Green synthesis is favored not only for its eco-friendly nature but also for its economic viability, scalability, and ability to produce biocompatible

*Corresponding Author: Hemangiben Sheth, Smt. S. M. Panchal Science College, Talod - 383215, Gujarat, India. E-mail: hemangisheth1998 @ gmail.com nanoparticles with enhanced functionality [4-6]. Among the various biological templates, algae have attracted particular interest due to their rapid growth rate, ease of cultivation, and rich repertoire of bioactive compounds – including proteins, polysaccharides, pigments, and antioxidants – that facilitate both the reduction of metal ions and stabilization of the resulting nanoparticles during synthesis [7]. Recent studies have highlighted how marine macroalgae can be effectively used in green synthesis approaches [8,9]. Earlier research has also played a key role in explaining how natural compounds in algae, such as phytochemicals, help in forming and stabilizing nanoparticles. These early findings continue to shape the direction of ongoing studies in this field [10].

AgNPs, in particular, exhibit strong antimicrobial, antioxidant, and anticancer properties, making them promising candidates for therapeutic and biomedical applications. Compared to other noble metals such as gold, silver is more cost-effective while offering comparable biological efficacy [11]. The synthesis of AgNPs using algal extracts takes advantage of the natural abundance of functional biomolecules in algal cells, which can reduce silver ions (Ag⁺) to elemental silver (Ag⁰), while also acting as capping and stabilizing agents [12,13]. Beyond their conventional biomedical uses, greensynthesized AgNPs hold significant potential in advanced applications such as targeted drug delivery, biosensing, medical imaging, wound healing, implant coatings, and immune therapies, owing to their

nanoscale size, large surface area, and surface plasmon resonance (SPR) properties [14]. In environmental domains, AgNPs are being investigated for water purification, pollutant degradation, and air filtration due to their catalytic and antimicrobial capabilities [15].

These diverse applications not only demonstrate the multifunctionality of AgNPs but also align closely with several United Nations Sustainable Development Goals under the 2030 Agenda. The biomedical potential of green-synthesized AgNPs from marine alga supports Goal 3: Good health and well-being through novel antimicrobial, antioxidant, and anticancer applications. The adoption of green nanotechnology reflects Goal 9: Industry, innovation, and infrastructure by offering an eco-friendly alternative to conventional synthesis. Using marine algae aligns with Goal 12: Responsible consumption and production by minimizing toxic chemical use, while sustainable harvesting practices contribute to Goal 14: Life below water by promoting conservation of marine resources [16].

Response surface methodology (RSM) has emerged as a valuable tool in nanobiotechnology, facilitating the efficient optimization of synthesis parameters with minimal experimental trials. It enables the systematic evaluation of variables such as pH, temperature, precursor concentration, extract concentration, and reaction time, all of which significantly influence the characteristics of AgNPs, including their size, shape, and stability [17]. RSM has been successfully applied to optimize the biosynthesis of AgNPs using plant extracts [17,18], bacteria [19,20], and other biological systems. However, its application in marine algae-mediated AgNP synthesis has been explored in only a limited number of studies.

In the present study, AgNPs were synthesized using the red macroalga *Scinaia moniliformis* J. Agardh, a species rich in bioactive compounds such as alkaloids, flavonoids, phenols, tannins, steroids, triterpenes, cardiac glycosides, and polysaccharides that act as natural reducing and stabilizing agents. The synthesis process was optimized using RSM, and the resulting nanoparticles were characterized using spectroscopic and microscopic techniques. Their antimicrobial, antioxidant, and anticancer activities were evaluated through *in vitro* assays to explore their potential for biomedical applications. This work highlights a sustainable, algae-based approach to nanomaterial synthesis and demonstrates the multifunctionality of AgNPs derived from a novel marine algal source.

2. MATERIALS AND METHODS

Algal samples were collected from Gaytri Shaktipith Beach, Devbhoomi Dwarka, Gujarat, India (22°14′16.97″ N; 68°57′41.72″ E) in February 2023. The samples were placed in plastic zipper bags after being rinsed with seawater. Fresh algal specimens were collected and taxonomically identified using a standard phycological handbook [21]. The chemicals and media used in the study were procured from HiMedia Laboratories and Merck. Nutrient agar, agar—agar, and the antibiotic streptomycin sulfate were purchased from HiMedia, while silver nitrate (AgNO₃) was obtained from Merck. The bacterial strains used in the antibacterial assays were obtained from the Department of Microbiology, The Maharaja Sayajirao University of Baroda, Gujarat, India.

2.1. Algal Extract Preparation and AgNPs Synthesis

Naturally dried biomass of *S. moniliformis* J. Agardh was ground into a fine powder and stored in an airtight container until further use. 10 g of the dried algal powder was added to 100 mL of deionized water in a 250 mL beaker and incubated at 60°C in a water bath for 30 min.

The resulting extract was filtered sequentially through Whatman No. 1 filter paper and a 0.2 μ m sterile membrane filter. The filtered algal extract was then used for the synthesis of AgNPs. For the reaction, the algal extract was mixed with a 1 mM AgNO₃ solution in a 1:10 (v/v) ratio and incubated at 60°C for 24 h under dark conditions [22].

2.2. Algal Mediated Synthesis of AgNPs and their Characterization

To improve the efficiency and yield of nanoparticle synthesis, key parameters such as the pH of the algal extract and the reaction temperature were optimized using RSM in Minitab software. The software generated 13 experimental conditions, each representing a unique combination of the selected variables. These conditions were systematically tested, and the results were analyzed to determine the optimal values for the most efficient synthesis of AgNPs.

Following optimization, the synthesized AgNPs were subjected to comprehensive physicochemical characterization. Ultravioletvisible (UV-Vis) spectroscopy was performed across a wavelength range of 300–700 nm to detect the surface plasmon resonance (SPR) characteristic of AgNPs. Fourier-transform infrared (FTIR) spectroscopy was used to identify functional groups involved in the reduction and stabilization processes, with spectra recorded between 400 and 4000 cm⁻¹. The crystalline structure of the nanoparticles was confirmed through X-ray diffraction (XRD) analysis, conducted over a scanning range of 3°–90° (2θ). High-resolution transmission electron microscopy (HR-TEM) was employed to examine the morphology, particle size distribution, and structural features of the synthesized AgNPs [20].

2.3. Bio-Potentials of AgNPs

2.3.1. Antioxidant activity

To evaluate the antioxidant potential of the synthesized AgNPs, a standard 2,2-diphenyl-1-picrylhydrazyl (DPPH) free radical scavenging assay was performed. 1 mL of AgNP solution (at concentrations ranging from 10 μg/mL to 100 μg/mL) and 1 mL of methanol (blank) were each mixed with 1 mL of freshly prepared DPPH solution and incubated at 37°C for 30 min in the dark. Following incubation, absorbance was measured at 570 nm using a UV-Vis spectrophotometer [23].

2.3.2. Antibacterial activity

The antibacterial activity of the synthesized AgNPs was evaluated following the method described by Thakor $\it et~al.$ [6]. Briefly, 10 mm wells were created in agar plates seeded with 100 μL of human pathogenic bacterial culture (1 \times 106 colony-forming unit/mL) using a sterile cork borer. Each well was loaded with 100 μL of different treatments: AgNP solution (1 mg/mL), sterile distilled water (negative control), and streptomycin solution (1 mg/mL; positive control). The plates were then incubated at 37°C for 24 h. After incubation, the zones of inhibition (ZOI) were measured using a zone measuring scale (HiMedia).

2.3.3. Cell culture and cytotoxicity assay

The michigan cancer foundation-7 (MCF-7) breast cancer cell line was obtained from the National Centre for Cell Science, Pune. Cells were cultured in Dulbecco's Modified Eagle Medium supplemented with 10% fetal bovine serum and 1% penicillin–streptomycin and maintained in a 5% CO₂ atmosphere at 37°C in a CO₂ incubator [24]. To evaluate cell viability and cytotoxicity, the MTT assay was performed. MCF-7 cells were seeded at a density of 50,000 cells/

well in 96-well plates and allowed to adhere overnight. The following day, the culture medium was replaced with fresh medium containing varying concentrations of AgNPs (0–100 μ g/mL), and cells were incubated for 24 h. After incubation, 20 μ L of MTT solution was added to each well, and the plates were further incubated in the dark for 4 h. Subsequently, the supernatant was removed, and the resulting purple formazan crystals were dissolved in 100 μ L of dimethyl sulfoxide. The optical density (OD) was measured at 595 nm using an Epoch spectrophotometer (BioTek). The percentage of cell cytotoxicity was calculated based on OD values, providing a quantitative measure of the nanoparticle-induced cytotoxic effects [25].

2.4. Statistical Analysis

Statistical analyses, including RSM, were carried out using Minitab software. Additional analyses such as calculation of means, standard errors, and analysis of variance (ANOVA) were performed using Microsoft Excel and the Statistical Package for the Social Sciences software. These tools facilitated the comprehensive evaluation and interpretation of the experimental data.

3. RESULTS AND DISCUSSION

3.1. Biosynthesis of AgNPs

The color of algal extract and AgNO₃ mixture was immediately changed from colorless to yellow, indicating the formation of nanoparticles within the mixture. After 24 h, the reaction color turned completely dark brown as reported by the other researchers. Then the variables were optimized using the RSM.

3.2. Optimization of AgNPs Synthesis using RSM

The synthesis of AgNPs was optimized using RSM by investigating two key independent variables: the pH of the algal extract and the reaction temperature. The experimental setup was structured according to Tables 1 and 2, with the absorbance of synthesized nanoparticles recorded at 420 nm. The collected data were processed using Minitab software to determine the optimal conditions for maximum nanoparticle yield. According to RSM analysis in Minitab, a total of 13 experimental formulations were designed and evaluated based on response factors, including initial pH of the algal extract and reaction temperature. The interactions between these parameters were analyzed using quadratic models, and statistical summaries of response variables are presented in Table 3. The lack-of-fit test was employed to assess discrepancies between predicted and actual values, while the coefficient of determination (R²) and the significance of the lack-of-fit test were also evaluated.

3.2.1. Diagnostic analysis

Figure 1 illustrates the diagnostic plots for AgNP production using the red alga *S. moniliformis* J. Agardh. The near-identical match between actual and predicted values in these figures confirms the robustness and accuracy of the model.

3.2.2. Effect of RSM on AgNPs synthesis

The quantitative influence of predictor factors on the response variable (absorbance at 420 nm) is represented by the full quadratic polynomial equation below. The equation demonstrates how variations in independent variables influence the response. With an $R^2 = 98.88\%$ closely aligning with the adjusted R^2 of 97.65%, the model exhibited a strong fit to the response variable. Regression analysis revealed a positive correlation between AgNPs synthesis and the initial pH of the algal extract as well as the reaction duration, indicating that increasing these parameters enhances nanoparticle production.

Table 1: Actual values of the factors and their corresponding coded level.

S. No.	Variables	Coded values			
		-1 (low)	0 (medium)	1 (high)	
1	Reaction temperature (°C)	37	48.5	60	
2	pH of the algal extract	5	7	9	

Table 2: Reaction conditions and their respective responses.

Run order	pH of the algal extract	Reaction temperature (°C)	Abs. at 420 nm
1	7	64.76346	1.01
2	5	37	0.291
3	9.828427	48.5	0.609
4	5	60	0.549
5	7	48.5	0.742
6	7	32.23654	0.392
7	7	48.5	0.742
8	9	37	0.397
9	7	48.5	0.742
10	7	48.5	0.742
11	4.171573	48.5	0.597
12	9	60	1.181
13	7	48.5	0.742

Table 3: Statistical summaries of analysis of variance.

Source	DF	Adj SS	Adj MS	F-value	P-value
Model	5	0.648707	0.129741	12.44	0.002
Linear	2	0.530122	0.265061	25.41	0.001
pН	1	0.071248	0.071248	6.83	0.035
Temp	1	0.458874	0.458874	43.99	0.000
Square	2	0.049417	0.024708	2.37	0.164
рН*рН	1	0.046065	0.046065	4.42	0.074
Temp*Temp	1	0.007291	0.007291	0.70	0.431
2-Way interaction	1	0.069169	0.069169	6.63	0.037
pH*Temp	1	0.069169	0.069169	6.63	0.037
Error	7	0.073027	0.010432		
Lack-of-fit	3	0.073027	0.024342	*	*
Pure error	4	0.000000	0.000000		
Total	12	0.721734			

^{*:} indicates that the Lack-of-Fit F-value and P-value could not be calculated due to absence of pure error.

ANOVA confirmed that the independent variables had a statistically significant effect (P < 0.05) on the response. In addition, predictor terms with P-values below 0.05 significantly contributed to the model's predictive accuracy [Table 3]. The contour (2D) and surface (3D) plots in [Figure 2a and b] effectively depict the interactions between independent variables and their impact on AgNPs synthesis.

The response optimization curve in [Figure 2c] identified optimal conditions for maximizing AgNPs production: A pH of 9.82 for the algal extract and a reaction temperature of 64.76°C. Under these conditions, RSM predicted the highest AgNPs yield with an absorbance of 1.249 at 420 nm. The synthesized nanoparticles were harvested by

centrifugation at 10,000 rpm for 10 min, followed by two washes with sterile double-distilled water. The purified nanoparticles were then resuspended in an equivalent volume and subjected to characterization using various analytical techniques.

3.3. Characterization Techniques

3.3.1. UV-Vis spectroscopy analysis

The formation and stability of AgNPs synthesized using *S. moniliformis* extract were monitored using UV–Vis spectroscopy at different time intervals. For the analysis, 1 mL of algal extract (pH 9.82) was mixed with 9 mL of 1 mM AgNO₃ and incubated at 64.76°C. SPR bands consistently appeared between 436 and 438 nm [Figure 3a], confirming successful nanoparticle formation. At 24 h, a moderate absorption peak at 437 nm (absorbance = 1.315) was observed, which gradually increased to 1.989 by 96 h, indicating enhanced synthesis and stabilization [Table 4]. No peak shift was noted even after 96 h, suggesting stable particle morphology. The reaction mixture was then

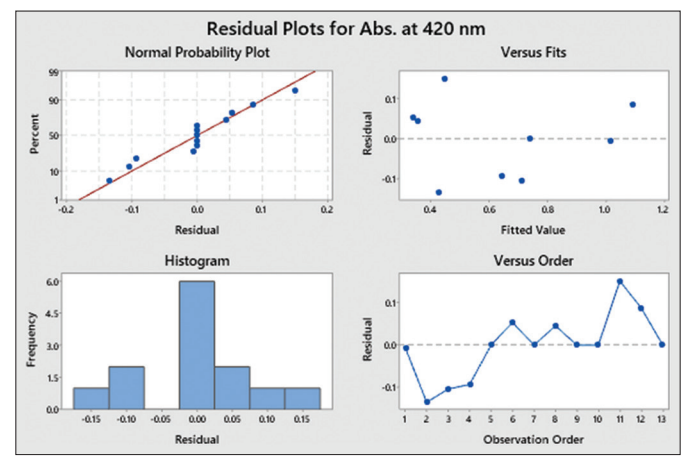


Figure 1: Diagnostic plot.

stored at room temperature, and after 185 days, the SPR band remained at 436 nm with a slightly increased absorbance of 2.017 – confirming long-term colloidal stability. The stable $\lambda_{\rm max}$ indicates uniform particle size and shape without aggregation, while increasing absorbance reflects a rise in AgNP concentration. Factors such as particle size, morphology, dielectric environment, and dispersion stability influence the SPR peak's position and intensity. The minimal shift in λ max and steady absorbance increase confirm controlled biosynthesis and high stability of AgNPs [5,6].

3.3.2. XRD analysis

XRD analysis was used to determine the crystalline structure and size of the synthesized AgNPs. The diffraction pattern displayed distinct peaks at 20 values [Figure 3b] corresponding to the (110), (111), (200), (220), and (311) planes, indicative of a face-centered cubic (FCC) structure (JCPDS No. 04–0783). The average crystallite size was calculated using the Debye-Scherrer equation $D=0.9k/\beta\cos\theta$, based on the full width at half maximum, Bragg's angle (θ), and X-ray wavelength (λ). The estimated crystallite sizes ranged from 2.03 to 14.09 nm, with a mean size of 7.23 \pm 2.02 nm [Table 5].

A sharp peak at approximately 37.89° (20), corresponding to the (111) plane, indicated a high degree of crystallinity. In addition to the main peaks, minor reflections were also observed, likely due to residual bioorganic compounds from the algal extract acting as capping agents. These findings align with previous studies on biosynthesized AgNPs using *Aspergillus brunneoviolaceus* [5] and the brown alga *Sargassum coreanum* [26], further confirming the FCC crystal structure and nanoscale dimensions of the particles.

3.3.3. FTIR spectroscopic analysis

FTIR analysis [Figure 3c] confirmed the presence of functional groups involved in the reduction and stabilization of AgNPs. A broad band at 3283 cm⁻¹ corresponds to O–H stretching, indicating phenolic and alcoholic compounds likely responsible for reducing Ag⁺ ions [6]. A peak at 1638 cm⁻¹ reflects C=O stretching, suggesting the role of

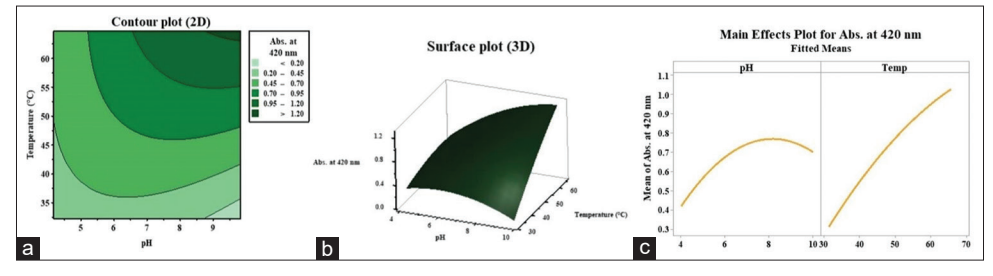


Figure 2: (a) Contour plot, (b) Surface plot, (c) Response optimization curve for silver nanoparticles production.

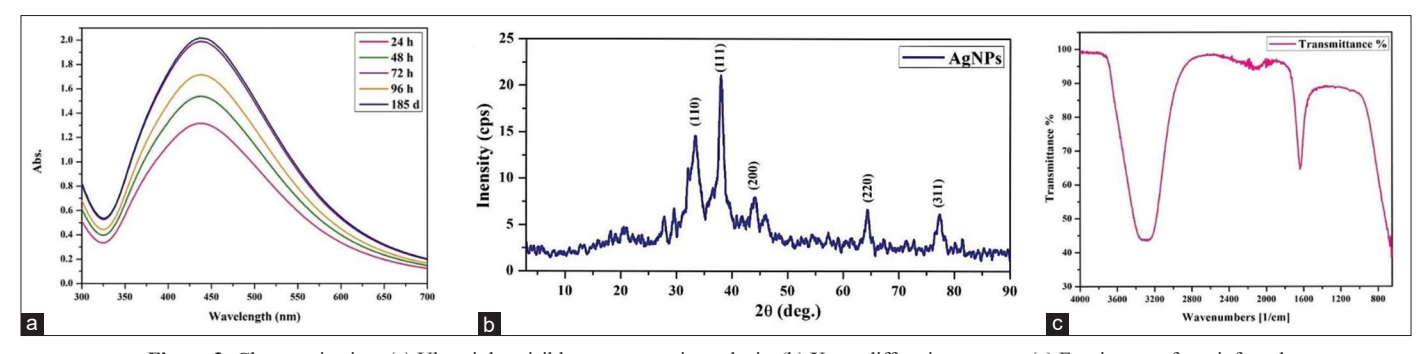


Figure 3: Characterization: (a) Ultraviolet-visible spectroscopic analysis, (b) X-ray diffraction pattern, (c) Fourier-transform infrared spectrum of silver nanoparticles.

carbonyl or amide groups, possibly from proteins, in capping the nanoparticles [22]. Minor peaks between 2104 and 2210 cm⁻¹ and at 2271 cm⁻¹ are attributed to C≡C stretching, indicating alkynecontaining phytochemicals like flavonoids or terpenoids. Bands in the 690–650 cm⁻¹ range suggest C–X stretching of alkyl halides [27]. These groups collectively support the dual function of the algal extract as a reducing and stabilizing agent. The involvement of proteinaceous compounds and amino acids in nanoparticle stabilization is consistent with previous FTIR-based studies [12,27].

3.3.4. TEM

TEM analysis provided detailed insights into the morphology and structure of the synthesized AgNPs. As shown in [Figure 4a and b], the HR-TEM image reveals that the nanoparticles are predominantly spherical. The particle size ranged from 5.05 to 61.4 nm, with an average diameter of 24.03 nm, indicating a well-distributed nanoscale population. These findings are further supported by the particle size distribution histogram [Figure 4d], which illustrates a narrow dispersion with most particles falling within the 10–40 nm range. The selected area electron diffraction pattern [Figure 4c] confirmed the FCC crystalline structure, characteristic of metallic silver. The observed interplanar spacing (~0.23 nm) corresponds to the (111) planes of FCC silver, in agreement with XRD results.

3.4. Biopotency of Synthesized AgNPs

3.4.1. Antioxidant activity

To evaluate the antioxidant potential of the synthesized AgNPs, a DPPH free radical scavenging assay was performed across a range of concentrations. The lowest scavenging activity was observed at $10\,\mu\text{g/mL}$ (18.31 \pm 3.02%), while the highest was recorded at $100\,\mu\text{g/mL}$ (98.60 \pm 0.37%). Statistical analysis using one-way ANOVA indicated a highly significant, dose-dependent increase in antioxidant activity (P < 0.0001; [Figure 5]). The IC $_{50}$ value was calculated as 41.09 \pm 0.35 $\,\mu\text{g/mL}$, highlighting the strong antioxidative efficacy of the biosynthesized AgNPs. Ascorbic acid was taken as the positive control and showed a steady rise in scavenging activity, from 20.44 \pm 2.43% at

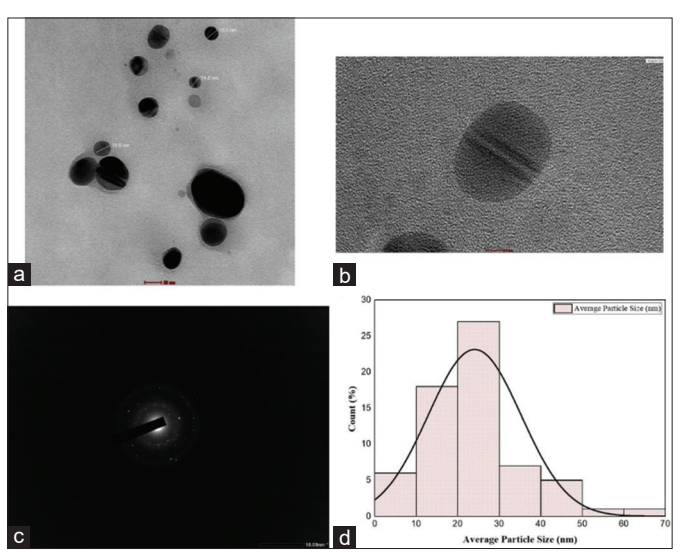


Figure 4: High-resolution transmission electron microscopy analysis of biosynthesized silver nanoparticles (AgNPs): (a) transmission electron microscopy (TEM) image at a scale of 20 nm; (b) TEM image at 5 nm scale revealing lattice fringes; (c) selected area electron diffraction pattern of AgNPs; (d) Particle size distribution histogram.

10 µg/mL to 99.12 \pm 0.40% at 100 µg/mL, confirming the reliability of the assay. At higher concentrations, the AgNPs displayed antioxidant activity that was almost comparable to ascorbic acid. These findings are consistent with earlier reports demonstrating concentration-dependent antioxidant responses in AgNPs synthesized from biological sources such as *Blighia sapida* [28] and *Azadirachta indica* [29] leaf extracts, as well as marine fungi including *Penicillium oxalicum* and *Fusarium hainanense* [6].

Table 4: UV-Vis spectroscopic data of AgNPs.

S/n	Reaction time	Peak intensity (Abs.)	λ_{\max} (nm)
1	24 h	437	1.315
2	48 h	438	1.537
3	72 h	438	1.715
4	96 h	437	1.989
5	185 day	436	2.017

UV-Vis: Ultraviolet-visible, AgNPs: Silver nanoparticles.

Table 5: Interpretation of data obtained by XRD analysis.

S. No.	2-theta	theta	FWHM	Crystallite size D (nm)	D nm (Average)	(hkl)
1	33.24	16.62	1.39	5.96	7.23 ± 2.02	110
2	37.89	18.945	1.58	5.32		111
3	43.2	21.6	4.2	2.03		200
4	65.5	32.75	0.67	14.1		220
5	77.2	38.6	1.16	8.76		311

XRD: X-ray diffraction, FWHM: Full width at half maximum.

Table 6: Antibacterial activity of AgNPs.

S. No.	Bacterial strains	AgNPs	Std. drug	AgNO ₃
1	Staphylococcus aureus	20.3 ± 0.33	28.0 ± 0.58	15.3 ± 0.33
2	Bacillus cereus	19.7 ± 0.33	30.3 ± 0.33	0.0 ± 0.0
3	Bacillus subtilis	21.0 ± 0.58	29.7±0.33	0.0 ± 0.0
4	Escherichia coli	27.3 ± 0.33	38.3 ± 0.33	15.0 ± 0.58
5	Klebsiella pneumoniae	24.7 ± 0.33	35.7 ± 0.33	12.3 ± 0.33
6	Shigella dysenteriae	25.3 ± 0.33	33.7±0.33	14.0 ± 0.58

AgNPs: Silver nanoparticles.

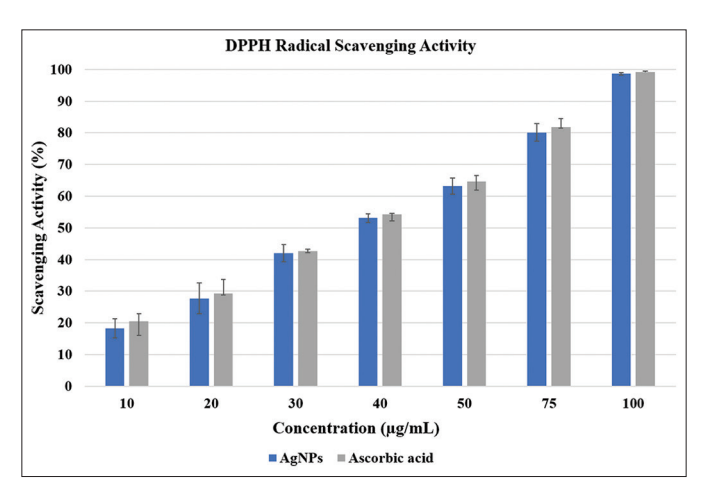


Figure 5: Antioxidative potency of silver nanoparticles.

3.4.2. Antibacterial activity

The antibacterial activity of algae-synthesized AgNPs was evaluated against various human pathogenic bacteria and compared with silver nitrate, sterile Milli-Q® water (negative control), and the standard antibiotic streptomycin. Antimicrobial efficacy was assessed by measuring the ZOI in millimeters (mm), presented as mean±standard error. *Escherichia coli* showed the highest sensitivity to AgNPs, with a ZOI of 27.3 ± 0.33 mm, followed by *Shigella dysenteriae* (25.3 ± 0.33 mm) and *Klebsiella pneumoniae* (24.7 ± 0.33 mm). *Bacillus cereus* was the least susceptible, exhibiting a ZOI of 19.7 ± 0.33 mm [Table 6]. One-way ANOVA followed by Tukey's honest significant difference test confirmed statistically significant differences among treatments (P < 0.0001). AgNPs exhibited significantly greater antibacterial activity than AgNO₃ (P < 0.001), although they remained less effective than the standard antibiotic (P < 0.001).

These results underscore the substantial antimicrobial potential of algae-derived AgNPs. While they do not outperform conventional antibiotics, they show superior efficacy over ionic silver and benefit from an eco-friendly synthesis route. Their enhanced activity may be attributed to their nanoscale dimensions and the presence of bioactive algal compounds, which could synergistically disrupt microbial membranes or promote reactive oxygen species (ROS) generation [30]. This highlights their potential as alternative or adjunct antimicrobial agents, especially against drug-resistant pathogens.

3.4.3. Anticancer activity

The cytotoxic potential of the synthesized AgNPs was evaluated against the human breast adenocarcinoma MCF-7 cell line using the MTT assay. Cells treated with increasing concentrations of AgNPs (10–100 µg) for 24 h demonstrated a clear, dose-dependent inhibition of cell viability. At the lowest tested dose (10 µg), a modest inhibition of $8.53 \pm 2.40\%$ was observed, indicating limited cytotoxicity. As the concentration increased, cell viability declined progressively, reaching $98.58 \pm 0.94\%$ inhibition at $100 \mu g$, indicating near-complete cytotoxicity and a strong dose–response relationship [Figure 6]. Statistical analysis using one-way ANOVA revealed a highly significant difference between treatment groups (F = 242.67, P < 0.0001), validating the observed trend.

The IC₅₀ value was determined to be $51.49 \pm 0.45 \,\mu g$ using a linear regression model (y = 1.0264×-2.8485), categorizing the AgNPs as a moderately potent cytotoxic agent. Interestingly, the standard drug 5-fluorouracil (5-FU) produced a comparable inhibition of $50.28 \pm 1.47\%$ at $40.7 \,\mu g$, placing AgNPs within the therapeutic efficacy range of a clinically used chemotherapeutic. Similar IC₅₀ values (30–70 $\,\mu g$ /mL) for green-synthesized AgNPs against MCF-7 cells

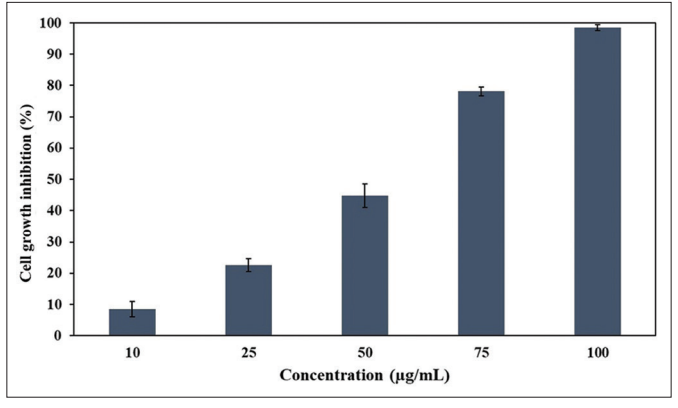


Figure 6: Cytotoxicity analysis of silver nanoparticles on MCF-7 cell line.

have been reported by Rajawat *et al.* [31]. Moreover, our findings are consistent with previous studies wherein AgNPs synthesized from the leaf extract of *Brassica oleracea* [32], red marine alga *Gracilaria foliifera* [33], and microalga *Coelastrella aeroterrestrica* [34] exhibited comparable cytotoxic effects against the MCF-7 cell line.

The observed cytotoxicity may be attributed to the disruption of mitochondrial dehydrogenase activity, as indicated by reduced MTT metabolism. The sharp decline in cell viability beyond 50 µg also suggests a threshold-dependent response. Given their comparable efficacy to 5-FU, these algal-derived AgNPs show promise as potential anticancer agents. However, additional studies involving other cancer models, non-cancerous cell lines, and mechanistic evaluations (e.g., apoptosis induction, ROS generation, or cell cycle arrest) are necessary to further validate their therapeutic potential and safety profile.

3.5. Mechanistic Insights, Limitations, and Future Directions

This study highlights *S. moniliformis* as a new and promising source for the green synthesis of AgNPs with significant biomedical potential. In the present work, only functional assays were carried out, and detailed mechanistic studies were not performed. Since AgNPs are reported to trigger ROS-mediated apoptosis in cancer cells [35] and show antibacterial activity through membrane disruption and interactions with key biomolecules [36], further investigations such as ROS assays, apoptosis marker analysis, flow cytometry, and ultrastructural studies will be necessary to clarify these mechanisms and to strengthen the biomedical significance of AgNPs derived from *S. moniliformis*.

4. CONCLUSION

This study successfully demonstrates the green synthesis of AgNPs using the red alga S. moniliformis through an eco-friendly, rapid, and costeffective approach. Optimization of synthesis parameters using RSM significantly enhanced nanoparticle yield, with optimal results achieved at pH 9.82 and 64.76°C. Characterization using UV-Vis spectroscopy, FTIR, XRD, and HR-TEM confirmed the formation of spherical, crystalline AgNPs with well-defined nanoscale dimensions and surface capping by bio-organic compounds derived from the algal extract. Functionally, the biosynthesized AgNPs exhibited potent biological activities. They demonstrated strong antioxidant capacity with a low IC₅₀ value of $41.09 \pm 0.35 \mu g$, indicating efficient free radical scavenging. Antibacterial assays revealed broad-spectrum activity against pathogenic bacteria, with efficacy surpassing silver nitrate and approaching that of standard antibiotics. Furthermore, the AgNPs showed significant anticancer potential against the MCF-7 breast cancer cell line, with a calculated IC_{so} of $51.49 \pm 0.45 \,\mu g$, closely comparable to the standard drug 5-fluorouracil. Taken together, these findings highlight the promise of algae-mediated AgNPs as multifunctional bio-nanomaterials with applications in antimicrobial therapy, oxidative stress mitigation, and cancer treatment. Further mechanistic investigations, along with in vivo studies, are essential to fully realize their clinical and therapeutic potential.

5. AUTHOR CONTRIBUTION

All authors made substantial contributions to conception and design, acquisition of data, or analysis and interpretation of data; took part in drafting the article or revising it critically for important intellectual content; agreed to submit to the current journal; gave final approval of the version to be published; and agree to be accountable for all aspects of the work. All the authors are eligible to be an author as per the International Committee of Medical Journal Editors (ICMJE) requirements/guidelines.

6. ACKNOWLEDGMENT

The authors gratefully acknowledge Smt. S. M. Panchal Science College, Talod (P.G. Centre in Botany and Department of Microbiology), as well as the Department of Biotechnology and the Department of Life Sciences of Hemchandracharya North Gujarat University, Patan, for providing the necessary research facilities.

7. FUNDING

This research did not receive any specific grant from funding agencies in the public, commercial, or not-for-profit sectors.

8. CONFLICTS OF INTEREST

The authors report no financial or any other conflicts of interest in this work.

9. ETHICAL APPROVALS

This study does not involve experiments on animals or human subjects.

10. DATA AVAILABILITY

All data supporting the findings of this study are available from the corresponding author upon reasonable request.

11. PUBLISHER'S NOTE

All claims expressed in this article are solely those of the authors and do not necessarily represent those of the publisher, the editors and the reviewers. This journal remains neutral with regard to jurisdictional claims in published institutional affiliation.

12. USE OF ARTIFICIAL INTELLIGENCE (AI)-ASSISTED TECHNOLOGY

The authors declare that they have not used artificial intelligence (AI)-tools for writing and editing of the manuscript, and no images were manipulated using AI.

REFERENCES

- Khan I, Saeed K, Khan I. Nanoparticles: Properties, applications and toxicities. Arab J Chem. 2019;12(7):908-31. https://doi. org/10.1016/j.arabjc.2017.05.011
- Dhaka A, Mali SC, Sharma S, Trivedi R. A review on biological synthesis of silver nanoparticles and their potential applications. Result Chem. 2023;6:101108. https://doi.org/10.1016/j.rechem.2023.101108
- Fahim M, Shahzaib A, Nishat N, Jahan A, Bhat TA, Inam A. Green synthesis of silver nanoparticles: A comprehensive review of methods, influencing factors, and applications. JCIS Open. 2024;16:100125. https://doi.org/10.1016/j.jciso.2024.100125
- Bhardwaj B, Singh P, Kumar A, Kumar S, Budhwar V. Ecofriendly greener synthesis of nanoparticles. Adv Pharm Bull. 2020;10(4):566-76. https://doi.org/10.34172/apb.2020.067
- Mistry H, Thakor R, Patil C, Trivedi J, Bariya H. Biogenically proficient synthesis and characterization of silver nanoparticles employing marine procured fungi Aspergillus brunneoviolaceus along with their antibacterial and antioxidative potency. Biotechnol Lett. 2021;43:307-16. https://doi.org/10.1007/s10529-020-03008-7
- 6. Thakor R, Mistry H, Patel H, Jhala D, Parmar N, Bariya H. Biogenic synthesis of silver nanoparticles mediated by the consortium comprising the marine fungal filtrates of *Penicillium oxalicum* and *Fusarium hainanense* along with their antimicrobial,

- antioxidant, larvicidal and anticancer potency. J Appl Microbiol. 2022;133(2):857-69. https://doi.org/10.1111/jam.15611
- Eze CN, Onyejiaka CK, Ihim SA, Ayoka TO, Aduba CC, Ndukwe JK, et al. Bioactive compounds by microalgae and potentials for the management of some human disease conditions. AIMS Microbiol. 2023;9(1):55-74. https://doi.org/10.3934/microbiol.2023004
- Choudhary S, Sangela V, Saxena P, Saharan V, Pugazhendhi A, Harish. Recent progress in algae-mediated silver nanoparticle synthesis. Int Nano Lett. 2023;13(3):193-207. https://doi.org/10.1007/s40089-022-00390-0
- Chaudhary R, Nawaz K, Khan AK, Hano C, Abbasi BH, Anjum S. An overview of the algae-mediated biosynthesis of nanoparticles and their biomedical applications. Biomolecules. 2020;10(11):1498. https://doi.org/10.3390/biom10111498
- Aziz E, Batool R, Khan MU, Rauf A, Akhtar W, Heydari M, et al. An overview on red algae bioactive compounds and their pharmaceutical applications. J Complement Integr Med. 2020;17(4). https://doi. org/10.1515/jcim-2019-0203
- Xu L, Wang YY, Huang J, Chen CY, Wang ZX, Xie H. Silver nanoparticles: Synthesis, medical applications and biosafety. Theranostics. 2020;10(20):8996-9031. https://doi.org/10.7150/thno.45413
- Chugh D, Viswamalya VS, Das B. Green synthesis of silver nanoparticles with algae and the importance of capping agents in the process. J Genet Eng Biotechnol. 2021;19(1):126. https://doi. org/10.1186/s43141-021-00228-w
- 13. Wu JY, Tso R, Teo HS, Haldar S. The utility of algae as sources of high value nutritional ingredients, particularly for alternative/complementary proteins to improve human health. Front Nutr. 2023;10:1277343. https://doi.org/10.3389/fnut.2023.1277343
- Laib I, Gheraissa N, Benaissa A, Benkhira L, Azzi M, Benaissa Y, et al. Tailoring innovative silver nanoparticles for modern medicine: The importance of size and shape control and functional modifications. Mater Today Bio. 2025;33:102071. https://doi.org/10.1016/j.mtbio.2025.102071
- Silva-Holguín PN, Garibay-Alvarado JA, Reyes-López SY. Silver nanoparticles: Multifunctional tool in environmental water remediation. Materials (Basel). 2024;17(9):1939. https://doi. org/10.3390/ma17091939
- United Nations. Transforming Our World: The 2030 Agenda for Sustainable Development. New York: United Nations; 2015. Available from: https://sdgs.un.org/2030agenda [Last accessed on 2025 Aug 11].
- Ibrahim M, Agboola JB, Abdulkareem AS, Adedipe O, Tijani JO. Optimization of green synthesis of silver nanoparticles using response surface method (RSM). IOP Conf Ser Mater Sci Eng. 2020;805(1):012022. https://doi.org/10.1088/1757-899X/805/1/012022
- Azmi SN, Al-Jassasi BM, Al-Sawafi HM, Al-Shukaili SH, Rahman N, Nasir M. Optimization for synthesis of silver nanoparticles through response surface methodology using leaf extract of *Boswellia sacra* and its application in antimicrobial activity. Environ Monit Assess. 2021;193(8):497. https://doi.org/10.1007/s10661-021-09301-w
- Ibrahim S, Ahmad Z, Manzoor MZ, Mujahid M, Faheem Z, Adnan A.
 Optimization for biogenic microbial synthesis of silver nanoparticles through response surface methodology, characterization, their antimicrobial, antioxidant, and catalytic potential. Sci Rep. 2021;11(1):770. https://doi.org/10.1038/s41598-020-80805-0
- Solís-Sandí I, Cordero-Fuentes S, Pereira-Reyes R, Vega-Baudrit JR, Batista-Menezes D, De Oca-Vásquez GM. Optimization of the biosynthesis of silver nanoparticles using bacterial extracts and their antimicrobial potential. Biotechnol Rep (Amst). 2023;40:e00816. https://doi.org/10.1016/j.btre.2023.e00816
- Jha B, Reddy CR, Thakur MC, Rao MU. Seaweeds of India: The Diversity and Distribution of Seaweeds of Gujarat Coast. Berlin: Springer Science and Business Media; 2009.
- Bhuyar P, Rahim MH, Sundararaju S, Ramaraj R, Maniam GP, Govindan N. Synthesis of silver nanoparticles using marine macroalgae *Padina* sp. and its antibacterial activity towards

- pathogenic bacteria. Beni Suef Univ J Basic Appl Sci. 2020;9:3. https://doi.org/10.1186/s43088-019-0031-y
- Khuda F, Jamil M, Khalil AA, Ullah R, Ullah N, Naureen F, et al. Assessment of antioxidant and cytotoxic potential of silver nanoparticles synthesized from root extract of Reynoutria japonica Houtt. Arab J Chem. 2022;15(12):104327. https://doi.org/10.1016/j.arabjc.2022.104327
- Reddy YP, Chandrasekhar KB, Sadiq MJ. A study of *Nigella sativa* induced growth inhibition of MCF and HepG2 cell lines: An antineoplastic study along with its mechanism of action. Pharmacognosy Res. 2015;7(2):193-7. https://doi.org/10.4103/0974-8490.150541
- Ghasemi M, Turnbull T, Sebastian S, Kempson I. The MTT assay: Utility, limitations, pitfalls, and interpretation in bulk and single-cell analysis. Int J Mol Sci. 2021;22(23):12827. https://doi.org/10.3390/ ijms222312827
- Somasundaram CK, Atchudan R, Edison TN, Perumal S, Vinodh R, Sundramoorthy AK, et al. Sustainable synthesis of silver nanoparticles using marine algae for catalytic degradation of methylene blue. Catalysts. 2021;11(11):1377. https://doi.org/10.3390/catal111111377
- Shankar A, Kumar V, Kaushik NK, Kumar A, Malik V, Singh D, et al. Sporotrichum thermophile culture extract-mediated greener synthesis of silver nanoparticles: Eco-friendly functional group transformation and anti-bacterial study. Curr Res Green Sustain Chem. 2020;3:100029. https://doi.org/10.1016/j.crgsc.2020.100029
- Akintola AO, Kehinde BD, Ayoola PB, Adewoyin AG, Adedosu OT, Ajayi JF, et al. Antioxidant properties of silver nanoparticles biosynthesized from methanolic leaf extract of Blighia sapida. Mater Sci Eng. 2020;805(1):012004. https://doi. org/10.1088/1757-899X/805/1/012004
- Kumari SA, Patlolla AK, Madhusudhanachary P. Biosynthesis of silver nanoparticles using *Azadirachta indica* and their antioxidant and anticancer effects in cell lines. Micromachines (Basel). 2022;13(9):1416. https://doi.org/10.3390/mi13091416
- Ibraheem IB, Abd-Elaziz BE, Saad WF, Fathy WA. Green biosynthesis
 of silver nanoparticles using marine Red Algae Acanthophora

- specifera and its antimicrobial activity. J Nanomed Nanotechnol. 2016;7(409):6. https://doi.org/10.4172/2157-7439.1000409
- Rajawat S, Kurchania R, Rajukumar K, Pitale S, Saha S, Qureshi MS. Study of anti-cancer properties of green silver nanoparticles against MCF-7 breast cancer cell lines. Green Process Synth. 2016;5(2):173-81. https://doi.org/10.1515/gps-2015-0104
- Ansar S, Tabassum H, Aladwan NS, Naiman Ali M, Almaarik B, AlMahrouqi S, et al. Eco friendly silver nanoparticles synthesis by Brassica oleracea and its antibacterial, anticancer and antioxidant properties. Sci Rep. 2020;10(1):18564. https://doi.org/10.1038/ s41598-020-74371-8
- Algotiml R, Gab-Alla A, Seoudi R, Abulreesh HH, El-Readi MZ, Elbanna K. Anticancer and antimicrobial activity of biosynthesized Red Sea marine algal silver nanoparticles. Sci Rep. 2022;12(1):2421. https://doi.org/10.1038/s41598-022-06412-3
- Hamida RS, Ali MA, Almohawes ZN, Alahdal H, Momenah MA, Bin-Meferij MM. Green synthesis of hexagonal silver nanoparticles using a novel microalgae *Coelastrella aeroterrestrica* strain BA_Chlo4 and resulting anticancer, antibacterial, and antioxidant activities. Pharmaceutics. 2022;14(10):2002. https://doi.org/10.3390/ pharmaceutics14102002
- Banerjee A, Qi J, Gogoi R, Wong J, Mitragotri S. Role of nanoparticle size, shape and surface chemistry in oral drug delivery. J Control Release. 2016;238:176-85. https://doi.org/10.1016/j. jconrel.2016.07.051
- Dakal TC, Kumar A, Majumdar RS, Yadav V. Mechanistic basis of antimicrobial actions of silver nanoparticles. Front Microbiol. 2016;7:1831.

How to cite this article:

Sheth H, Jha C. Eco-friendly fabrication of silver nanoparticles from the red macroalga *Scinaia moniliformis* and evaluation of their biomedical activities. J Appl Biol Biotech 2026;14(1):135-142. DOI: 10.7324/JABB.2025.259214